Revisiting the Probability Distribution of Low Streamflow Series in the United States

Shumaila J. Bhatti[1]; Charles N. Kroll, Ph.D., P.E.[2]; and Richard M. Vogel, Ph.D., M.ASCE[3]

Abstract: Droughts result in billions of dollars in annual losses, loss of life, and the displacement of people. The characterization of hydrologic drought enhances the prediction of streamflow statistics that are important for various water resource applications. L-moments were used to examine the goodness of fit of selected 3-parameter probability distributions to the low streamflow series at 704 unregulated gaged rivers in the contiguous United States. Stream gages with and without zero flows were identified, and the use of the inverse transformation of nonzero low flows and censoring of both tails of the distribution were explored. Overall, the log-Pearson type III (LP3), 3-parameter lognormal (LN3), and Pearson type III (PE3) all appear to be acceptable distributions for describing the low streamflow series in the United States at sites with no zero low flows. For the inverse flows, the Generalized Extreme Value (GEV) distribution also performed well, while censoring did not improve the ability to distinguish between distributions. **DOI: 10.1061/(ASCE)HE.1943-5584.0001844.**

Author keywords: Hydrologic drought; L-moments; Low streamflow series; Probability distribution; Frequency analysis; Censor; Inverse streamflow.

Introduction

Droughts are some of the costliest disasters in the world, resulting in huge economic losses, the displacement of people, and loss of life (FAO 2017; NOAA-NCEI 2018). For example, the 2015 drought in California incurred a total loss of $2.74 billion with $1.84 billion due to direct agricultural losses (Howitt et al. 2015). The reoccurrence of drought throughout the world makes improving the characterization and frequency analysis of low streamflow particularly important.

The American Meteorological Society (AMS) identifies four categories of drought: meteorological, agricultural, hydrologic, and socioeconomic (AMS 1997). Hydrologic drought is caused by water shortages in the hydrologic system, which includes surface or subsurface water in the form of streamflow, groundwater, reservoirs, and lakes. Measures of hydrologic drought are useful for water quality management, the issuance and renewal of discharge permits, planning for hydropower, water supply, navigation, cooling and irrigation systems, and to assess the impacts of prolonged droughts on the ecosystem (Smakhtin 2001; Kroll and Vogel 2002; VanLoon 2015; Zou et al. 2018).

Hydrologic drought is often characterized by low streamflow statistics. Common low streamflow statistics include the 7-day, 10-year low streamflow (7Q10), which is the 7-day annual minimum streamflow with a nonexceedance probability of 10% (Riggs 1980), and the daily streamflow with an exceedance probability of 95% (Q95) (Smakhtin 2001). Other common low streamflow statistics employed in practice include the 7Q2, 30Q10, 30Q2, Q99, and Q90 (Hughes 1981; Armentroutand and Wilson 1987; Zalants 1992; Atkins and Pearman 1995; Smakhtin 2001). To estimate the 7Q10 from a historical streamflow record, a probability distribution is fit to the 7-day annual minimum streamflows and the 10th percentile of that distribution is used as the estimate of the 7Q10 (Vogel and Kroll 1989; Smakhtin 2001; Gao et al. 2017). Similar techniques are used to estimate the 7Q2, 30Q10, and 30Q2. In the US, the log-Pearson type 3 distribution (LP3) is generally used to describe low streamflow series and estimate low streamflow statistics (Barnes 1986; Tasker 1989), though use of the LP3 for low streamflows is based on its recommendation for describing annual maximum instantaneous flows (Rossman 1990; Griffis and Stedinger 2007; England et al. 2018). Other probability distributions have sometimes been recommended for describing low streamflow series (Pearson 1995; Vogel and Wilson 1996; Kroll and Vogel 2002).

Numerous studies have used L-moments for fitting and assessing the ability of different probability distributions to describe low streamflow series (Pearson 1995; Vogel and Wilson 1996; Kroll and Vogel 2002; Modarres 2008; Chen et al. 2010; Peng et al. 2010; Dodangeh et al. 2011; Wang et al. 2011; Dodangeh et al. 2013; Keshtkar 2015). L-moments are popular because they: (1) are robust in the presence of outliers, (2) perform well for small sample sizes, (3) are able to characterize a wide range of distributions, (4) are nearly unbiased for all underlying distributions, and (5) are preferable to product moments for highly skewed data (Vogel and Fennessey 1993; Hosking and Wallis 1997; Sankarasubramanian and Srinivasan 1999).

The most commonly recommended probability distributions for describing low streamflow series include the Generalized Extreme Value (GEV), Generalized Logistic (GLO), Generalized Pareto (GPA), 3-parameter lognormal (LN3), log-Pearson type III (LP3), Pearson type III (PE3), and 3-parameter Weibull distribution (WEI) (Chowdhury et al. 1991; Guttman et al. 1993; Kroll and Vogel 2002; Peng et al. 2010; Blum et al. 2017). Some previous studies have used large data sets and L-moments to identify the best distributions to describe low streamflow series; these studies have

[1]Ph.D. Student, Dept. of Environmental Science, State Univ. of New York College of Environmental Science and Forestry, Syracuse, NY 13210. Email: bhattisj90@gmail.com

[2]Professor, Dept. of Environmental Resources Engineering, SUNY ESF, Syracuse, NY 13210 (corresponding author). Email: cnkroll@esf.edu

[3]Research Professor, Dept. of Civil and Environmental Engineering, Tufts Univ., Medford, MA 02478. Email: richard.vogel@tufts.edu

Note. This manuscript was submitted on October 27, 2018; approved on May 25, 2019; published online on August 8, 2019. Discussion period open until January 8, 2020; separate discussions must be submitted for individual papers. This paper is part of the ***Journal of Hydrologic Engineering***, © ASCE, ISSN 1084-0699.

generally not reached a consensus on the best distribution to employ (Pearson 1995; Vogel and Wilson 1996; Kroll and Vogel 2002).

Pearson (1995) studied the regional frequency distribution patterns of low flows (1-day, 7-day, and 30-day minimum averages) of nearly 500 catchments in New Zealand. Based on a visual inspection of their L-moment diagrams and the expected spread of the sample L-moments, Pearson concluded that no single 2- or 3-parameter distribution provided an adequate fit across all sites; however, Pearson generally recommended the GLO, GEV, LN3, and PE3 distributions. Vogel and Wilson (1996) used the USGS Hydro-Climatic Data Network (HCDN) sites (Lin 2012) that originally consisted of 1,570 streamflow sites with minimal anthropogenic influences. These sites were employed to study the probability distribution of annual maximum, mean, and minimum flows using L-moments to assess the goodness of fit; it was concluded that the PE3 distribution provides the best fit for both the annual minimum and annual average streamflow. Kroll and Vogel (2002) used 1,505 HCDN sites to identify potential probability distributions for describing 1-, 7-, and 30-day annual low flow minimums. Kroll and Vogel concluded that even when considering many sites across a large region, it is hard to distinguish probability distributions using L-moments and that L-moments followed different trends at intermittent and nonintermittent sites. For nonintermittent sites, the LN3 distribution was suggested and for intermittent sites, the PE3 distribution was suggested.

Some studies have shown the importance of data transformations when examining low flow series (Hosking 1995; Farmer et al. 2015). Farmer et al. (2015) recommended the use of inverse moments or negative moment orders for low flow series because the positive moment orders do not effectively capture the probabilistic lower tail behavior of flows above a certain exceedance probability. This study explores the distribution of the inverse of the annual minimum series (fitting 1/X as opposed to X, where X is the annual minimum series). In addition to the benefits described by Farmer et al. (2015), this transformation removes the chance of estimating negative low flow quantiles for real-space probability distributions, which can be a problem in practice. Hosking (1995), Zafirakou-Koulouris et al. (1998), and Kroll and Vogel (2002) employed L-moments for left censored samples. Typically, left censored L-moments have been employed to handle low flow series that contain zeros (Kroll and Vogel 2002). Unusually large observations might influence the distributional fit to the lower tail of the distribution. For flood frequency analyses in the United States, a multiple Grubbs-Beck test (Cohn et al. 2013) is recommended to identify potentially influential low flood observations (England et al. 2018). This is typically done on a site-by-site basis. In a fashion analogous to the process employed [what is done] for flood frequency, the present research explores the censoring of a certain percentage of the upper tail of the distribution and examines whether such censoring may help us better distinguish between potential 3-parameter probability distributions.

Since Kroll and Vogel (2002), there has not been another study, to the authors' knowledge, that has assessed the goodness of fit of different probability distributions to low streamflow series across the conterminous US. The aim of this study is to identify appropriate probability distributions for low streamflow series in the conterminous US using L-moments for a new subset of unregulated basins (HCDN-2009) to see if probability distributions may better fit the inverse of these series and to see if the distributional fit can be improved by fitting a lower percentage of the data set using censored L-moment diagrams.

Study Area and Streamflow Data

Fig. 1 shows the location of the 704 streamflow gages employed in this analysis. These gaged sites are from the USGS's Hydro-Climatic Data Network 2009 (HCDN-2009). This database was selected because these sites have minimal anthropogenic impacts and are generally able to reflect natural hydrologic conditions (Lin 2012; Gao et al. 2017). For the purpose of this study, all records in the HCDN-2009 data set have been extended up to the 2017 water year. Table 1 contains summary statistics for the streamflow sites employed in this study (Falcone 2011). Record lengths at these sites ranged from 22 to 115 years, with a median record length of 63 years, while the drainage areas ranged from 2.2 to 25,800 km^2, with a median of 325 km^2. At each site, a low flow water year was defined as April 1 to March 31, as most low streamflows in the US generally occur in the late summer or early fall (Kroll and Vogel 2002). At each site for every continuous water year, the following low flow series were estimated: 1-day, 3-day, 7-day, and 30-day annual minimums, and 90% (Q90), 95% (Q95), and 99% (Q99) annual flow duration curve exceedance probabilities.

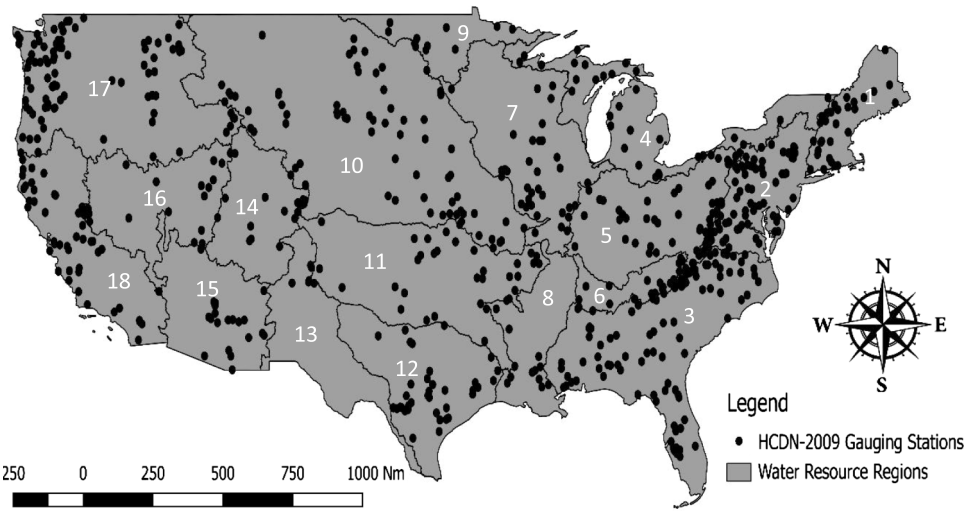

Fig. 1. Location of 704 HCDN-2009 gaging stations in the contiguous US.

Table 1. Summary statistics of 704 HCDN-2009 streamflow gaging stations and pertinent watershed characteristics

Characteristic	Minimum	Maximum	Median	Mean
Record length (years)	22	115	62	63.4
Drainage area (km^2)	2.2	25,800	325	795
Average basin precipitation (cm)	26.0	403	112	117
Average basin temperature (°C)	−1.7	22.6	10.1	10.3
Potential evapotranspiration (mm/year)	306	1,190	650	681
Snow percent of total precipitation (percent)	0	88.4	14.7	20.7
Streams density (km/km^2)	0.09	1.42	0.75	0.75
Maximum Strahler order in watershed	1	11	4	3.83
Sinuosity of mainstem streamline	1.03	5.14	1.51	1.61
Baseflow index (percent)	1.6	85.4	46.4	45.9
Watershed annual runoff (mm/year)	1	3,730	389	486
Elevation at gauge location (m)	0	3,190	283	540

Source: Data from Falcone (2011).

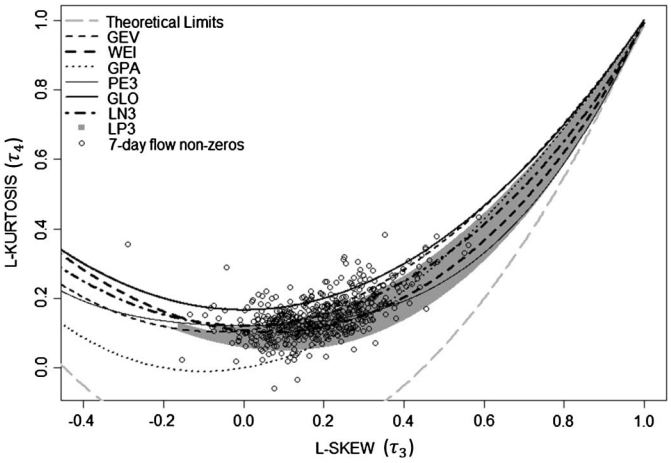

Fig. 2. τ_3 versus τ_4 for 7-day annual minimum flows at HCDN-2009 sites with no zeros.

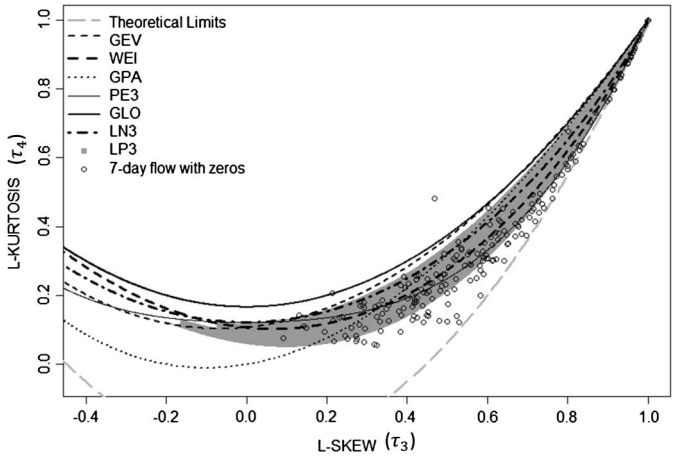

Fig. 3. τ_3 versus τ_4 for 7-day annual minimum flows at HCDN-2009 sites with zeros.

L-Moment Diagrams

L-moment diagrams provide a visual tool to compare sample L-moment ratios to theoretical L-moment ratio relationships for different probability distributions (Stedinger et al. 1993). A relationship between L-moment ratios exists for various probability distributions and for most 3-parameter probability distributions, a unique relationship generally exists between τ_3 (L-skew) and τ_4 (L-kurtosis) (Hosking and Wallis 1997). Low flow processes are complex, influenced by factors such as climatology, hydrogeology, and geomorphology, and a 2-parameter distribution is unlikely to capture the variety of distributional shapes of the low flow series, especially over a large area (Kroll and Vogel 2002). Distributions with more than 3 parameters (e.g., kappa and Wakeby) are not considered here. If a data series is described by a specific 3-parameter probability distribution, one expects sample τ_3 and τ_4 estimates to cluster around the theoretical τ_3:τ_4 relationship for that 3-parameter distribution. Vogel and Fennessey (1993) showed that L-moment ratio diagrams are always preferred to product moment ratio diagrams for analyzing the goodness of fit of a probability distribution to observations. Hosking and Wallis (1997) provided a thorough description of the estimation of sample L-moment ratios and the theoretical L-moment ratio relationships for different probability distributions.

At each site, for each low streamflow series, the sample L-moment ratios were estimated using the lmom package in R (Hosking 2017). For each distribution, the theoretical relationship between τ_3 and τ_4 was obtained from the literature. The τ_3:τ_4 relationship for the GEV, GPA, GLO, LN3, and PE3 distributions can be found in Hosking and Wallis (1997). The τ_3:τ_4 relationship for the WEI distribution can be found from a GEV distribution (if X ~ GEV, −X ~ WEI) or in Goda et al. (2011). Unlike the other 3-parameter distributions, the τ_3:τ_4 relationship for the LP3 distribution is represented by an area as opposed to a line (Griffis and Stedinger 2007). Here, the LP3 region for a log skew between −1.4 and 1.4 approximated by Griffis and Stedinger (2007) is used for the LP3 distribution.

One important issue with low streamflow series is the presence of flows recorded as zero within the record. Kroll and Vogel (2002) showed that the L-moment ratios of low flows at such intermittent streamflow sites often exhibited different characteristics than the L-moment ratios at nonintermittent streamflow sites. Here, sites with streamflow series including zeros were identified and L-moment diagrams were developed for sites with and without zeros.

L-Moment Diagrams for Untransformed Flows

Figs. 2 and 3 present the sample estimates of τ_4 versus τ_3 for 7-day annual minimum low streamflows in the contiguous US for 495 sites without zero 7-day minimums and 209 sites with zero 7-day annual minimums, respectively. These plots also include the τ_3:τ_4

Table 2. Goodness of fit results for 7-day annual minimum flow without zero, with zeros, and inverse of nonzeros for the contiguous US

	Nonzero			Inverse			With Zeros		
Distribution	NSE	Bias	AWAD	NSE	Bias	AWAD	NSE	Bias	AWAD
LP3	0.805	0.0109	0.0126	0.957	0.0153	0.0161	0.981	−0.006	0.0093
LN3	0.431	−0.0102	0.0366	0.900	0.0039	0.0385	0.774	−0.0688	0.0733
PE3	0.345	0.0102	0.0381	0.790	0.0343	0.0546	0.924	−0.0077	0.0351
GEV	0.324	−0.0177	0.0404	0.906	−0.0114	0.0375	0.544	−0.108	0.111
WEI	0.297	0.0228	0.0389	0.824	0.0391	0.0508	0.902	−0.0269	0.0433
GLO	−0.395	−0.0563	0.0621	0.826	−0.0431	0.0543	0.477	−0.119	0.121
GPA	−1.01	0.0687	0.0726	0.709	0.0648	0.0704	0.749	−0.0619	0.0755

relationships for the GEV, WEI, GPA, PE3, GLO, LN3, and LP3 distributions.

Based on visual assessment, sites with nonzero 7-day annual minimum flows appear to be best represented by the LP3 distribution, though many of the observed data points fall above the LP3 area (a higher kurtosis for a specific value of skew). The PE3, GEV, or LN3 appears to be the second-best distribution. This analysis, though, favors the LP3 distribution, which is presented by an area for a range of log space skew from −1.4 to 1.4. As the true skew is unknown, this potential area is represented as a gray shaded region in Figs. 2 and 3. For sites with 7-day low flow minimums with zeros shown in Fig. 3, the LP3 also appeared to provide the best fit, while the PE3 may be the second-best distribution; on this figure, the observed data points generally fall below the LP3 area and P3 curve (a lower kurtosis for a specific value of skew).

To avoid a visual assessment of goodness of fit based on visual inspection of the L-moment diagrams, a number of more quantitative metrics were also calculated to assess the goodness of fit of probability distributions to the sample L-moment ratios. Various tests and indices have been used as a measure of distributional goodness of fit. These include the Kolmogorov-Smirnov test (Chowdhury et al. 1991; Caruso 2000), the chi-squared test (Caruso 2000), probability plot correlation coefficient tests (Filliben 1975; Vogel and Kroll 1989), and an L-moment average weighted distance (Kroll and Vogel 2002; Yue and Wang 2004; Kim et al. 2010). Many regional L-moment studies have also used Z^{DIST}, the Hosking and Wallis (1997) regional goodness of fit statistic (Pearson 1991; Hosking and Wallis 1993; Yue and Wang 2004; Modarres 2008; Chen et al. 2010; Peng et al. 2010; Dodangeh et al. 2011; Hussain 2011; Dodangeh et al. 2013; Hussain 2017), though this approach assumes all series are generated from a parent distribution with the same τ_4, which is unlikely for low streamflows series distributed across the conterminous US.

For a 3-parameter distribution, the first three L-moments would be determined by and thus fixed by the fitted parameters of the given distribution. However, the fourth L-moment and therefore τ_4 would be freely determined by the fitted distribution. The quantitative metrics used here are based on comparing the sample τ_4 to a distribution's theoretical value of τ_4 corresponding to the value of the sample τ_3. A record-length weighted Nash-Sutcliffe efficiency (NSE), bias, and average weighted absolute deviation (AWAD) are examined as the goodness of fit statistics:

$$NSE = 1 - \frac{\sum_{i=1}^{N} n_i(\tau 4_{S,i} - \tau 4_{D,i})^2}{\sum_{i=1}^{N} n_i(\tau 4_{S,i} - \overline{\tau 4}_S)^2} \quad (1)$$

$$Bias = \frac{\sum_{i=1}^{N} n_i(\tau 4_{S,i} - \tau 4_{D,i})}{\sum_{i=1}^{N} n_i} \quad (2)$$

$$AWAD = \frac{\sum_{i=1}^{N} n_i|\tau 4_{S,i} - \tau 4_{D,i}|}{\sum_{i=1}^{N} n_i} \quad (3)$$

where N = number of sites, $\tau 4_{S,i}$ = at-site τ_4 at the ith site, $\tau 4_{D,i} = \tau_4$ of the respective probability distribution at the value of the at-site τ_3 at site i, $\overline{\tau 4}_S$ = weighted mean of the at-site L-kurtosis across all sites, and n_i = number of years of record at site i. Here, the NSE is calculated with the at-site estimate of τ_4 in the denominator as opposed to the value of τ_4 resulting from the fitted distribution. If the fitted distributional value of τ_4 was used, the denominator would change for every distribution and distributions where the fitted distributional τ_4 had a larger variance would generally be favored. Here, the NSE of every distribution is scaled similarly by the weighted sum of squares of the at-site τ_4 ($\tau 4_{S,i}$) from its mean ($\overline{\tau 4}_S$). The resulting value of NSE measures how the distribution fits the data as opposed to how the data fits the distribution. If the NSE is closer to 1, the fit of the probability distribution is better. An unbiased estimator has a bias of 0; hence, the closer bias is to 0, the better the fit. While NSE and bias are common metrics of goodness of fit, each does not completely describe performance. A few observations far from the mean of the distribution could create a large reduction in NSE, even when the overall fit is good. If the observations are far from the mean, but equally distributed around the mean, the bias may be close to 0, even though the fit is not particularly good. To balance these metrics, the AWAD is also used, which weights underestimation and overestimation equally. The smaller the AWAD, the better the performance of the distribution (Kroll and Vogel 2002).

Table 2 contains the results for the NSE, bias, and AWAD for the 7-day annual minimum low flow series for sites with no 7-day minimum of zero (from Fig. 2) and sites with zeros (from Fig. 3). Distributions have been put in order based on the NSE of the nonzero 7-day annual minima. Sites with more than 90% of the 7-day annual minimums recorded as zero produced unusually large L-moment ratios; these sites were not included in the calculations in Table 2 of the performance metrics for sites with zeros. For the LP3 distribution, if $\tau 4_{S,i}$ was within the shaded region in Figs. 2 and 3, it was assumed to be equal to $\tau 4_{D,i}$; for values outside of this area, $\tau 4_{D,i}$ was taken as the upper limit (for larger $\tau 4_{S,i}$) or lower limit (for smaller $\tau 4_{S,i}$) of the shaded area at the value of the at-site τ_3.

On the basis of the values of the NSE, bias, and AWAD in Fig. 2 for the nonzero 7-day low flow series, the LP3 provides the best fit; however, the LN3 and PE3 also seem to be plausible distributions, especially considering the fact that the approach to evaluating LP3 differs significantly from the approach to evaluating all other distributions considered. To examine the relative performance of different distributions for different flow series, a performance metric was calculated for each goodness of fit statistic:

$$Performance\ Ratio_{NSE} = \frac{NSE_{distribution}}{NSE_{best\_distribution}} \quad (4)$$

$$Performance\ Ratio_{Bias} = \frac{|Bias_{best\_distribution}|}{|Bias_{distribution}|} \quad (5)$$

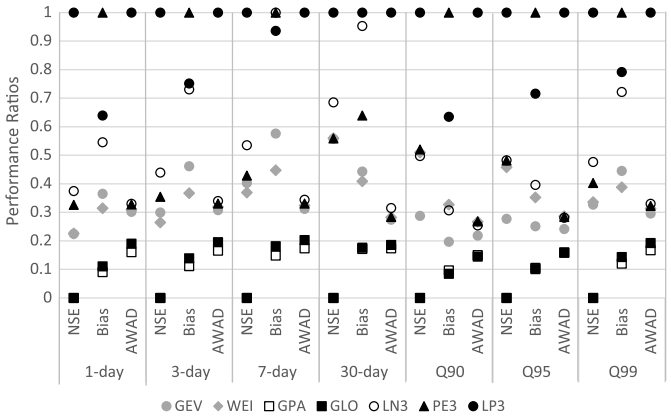

Fig. 4. Distributional performance ratios for low streamflow series with no zero flows for the 1-day, 3-day, 7-day, 30-day, Q90, Q95, and Q99 annual minimum series.

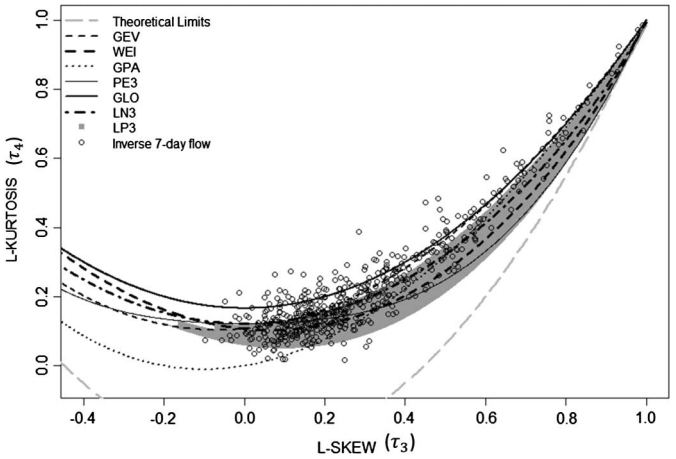

Fig. 5. τ_3 versus τ_4 for the inverse 7-day annual minimum flows at HDCN-2009 sites with no zeros.

$$Performance\ Ratio_{AWAD} = \frac{AWAD_{best\_distribution}}{AWAD_{distribution}} \quad (6)$$

where $NSE_{best\_distribution}$ = NSE for the distribution with the highest NSE, $Bias_{best\_distribution}$ = bias for the distribution with the smallest absolute value of the bias, and $AWAD_{best\_distribution}$ = AWAD for the distribution with the smallest AWAD. The performance ratio will be 1 for the best distribution and lower than 1 for distributions that are not the best. Note that when $Bias_{best\_distribution}$ is close to 0, the performance ratios of the other distributions are generally very low.

Fig. 4 shows the distributional performance ratios for the 1-day, 3-day, 7-day, and 30-day low flow series, as well as for the annual Q90, Q95, and Q99 series, at sites with no zero flows. When a distribution produced a negative NSE and thus a negative performance ratio, they were plotted as 0 in Fig. 4. In general, the LP3, LN3, and PE3 are always the most plausible distributions regardless of the flow series. Of the other 3-parameter distributions considered, the GEV generally performed better than the WEI, and the GLO and GPA performed worse than all other distributions. The GEV, GLO, LN3, and PE3 were proposed by Kroll and Vogel (2002), Pearson (1995), and Vogel and Wilson (1996) for fitting low streamflow series and the results of this study are generally consistent with their findings, though favor the LP3, LN3, and PE3 over the GEV and GLO distributions. Vogel and Wilson (1996) and Kroll and Vogel (2002) also examined low flow minimums for the HCDN sites (though a different subset of sites). Vogel and Wilson (1996) suggested the PE3 for the annual minimum low flow series and Kroll and Vogel (2002) recommended the LN3 for intermittent sites and the PE3 for nonintermittent sites. The LP3 is recommended for flood flow frequency analyses with US federal guidelines (England et al. 2018) and from the results presented here, the LP3 appears to be a flexible distribution that generally also provides a good fit to the low streamflow series.

From Table 2, for sites with 7-day annual minimums containing zeros, the LP3 again provided the best fit, while the PEI and WEI provided plausible fits to these series. The GLO and GEV distributions produced a drop-off in performance and thus are less plausible for describing 7-day annual minimums with zeros. Though not shown here, similar results were obtained for 1-day, 3-day, and 30-day low flow series. For the annual Q90, Q95, and Q99 series with zeros, the LP3 again provided the best fit, and the PE3 and WEI also were plausible distributions. As expected, the at-site τ_3 and τ_4 estimates increase as more zeros are present in the record due to a truncation of the lower tail of the distribution (note these results are not presented in this paper).

L-Moment Diagrams of Inverse Flows

It has been proposed that for low flow series, employing inverse moments might improve the characterization of these series (Farmer et al. 2015). Here, an assessment was made of whether probability distributions provide a better fit to the inverse transformation of the flow series (i.e., $1/X$) than to the original untransformed flow series (i.e., X). By taking the inverse transformation, the smaller flows that were originally in the lower tail of the distribution are now the largest observations and thus are in the upper tail of the distribution. Taking an inverse transformation removes the chance of estimating negative quantiles for real-space probability distributions, which can be a problem in practice.

Fig. 5 presents the sample estimates of τ_4 versus τ_3 for the inverse 7-day annual minimum low streamflow in the contiguous U.S. for the 495 sites without zero 7-day minimums. The plot also includes the τ_3:τ_4 relationship for the GEV, WEI, GPA, PE3, GLO, LN3, and LP3 distributions. The at-site L-moment ratios in Fig. 5 for the inverse low flows have a wider range of τ_3 and τ_4 than the plot of the untransformed flows (Fig. 2).

Table 2 also presents performance metrics for the inverse of the nonzero low flow series. For the 7-day inverse low flows, the LP3 again performs best with the highest NSE and low bias and AWAD values. The GEV and LN3 also appear to be plausible distributions for the inverse low flow series. Importantly, for all distributions, the NSE for the inverse flows is significantly larger than the NSE for the untransformed flow series, though the AWAD and bias are of similar magnitude. The larger variance in the at-site τ_4 for the inverse flows compared to the untransformed flows would inflate the NSE [an increase in the denominator in Eq. (1)]. Overall, the fit of probability distributions to the inverse flows appears as good as the fit of the untransformed low flows.

Fig. 6 shows the distributional performance ratios for the inverse flow series corresponding to the 1-day, 3-day, 7-day, and 30-day low flow series, as well as for the annual Q90, Q95, and Q99 series at sites with no zeros. Similar to the preceding results provided in Fig. 4 for the untransformed flow series, for the inverse flow series, the LP3, LN3, and possibly the GEV distribution appear to be plausible distributions for describing a wide array of low flow series in the US.

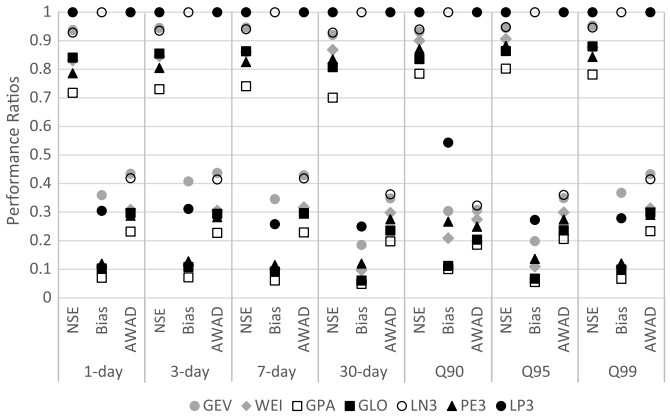

Fig. 6. Distributional performance ratios for the inverse low streamflow series with no zero flows for the 1-day, 3-day, 7-day, 30-day, Q90, Q95, and Q99 annual minimum series.

L-Moments Within Water Resource Regions

Across the conterminous US, there is a wide range of climatic, geologic, geomorphic, and topographic conditions that impact low streamflow processes. Of interest was whether the LP3, LN3, and PE3 distributions would still be preferred if results were partitioned based on the USGS Water Resource Regions identified in Fig. 1. Fig. 7 is similar to Figs. 4 and 6, but is for the untransformed 7-day annual minimum flows for each of the 18 USGS Water Resource Regions. In terms of the NSE and AWAD, the LP3 is the best distribution regardless of the region, with the LN3 and PE3 generally being the next most plausible distributions. Fig. 8 presents the same results as Fig. 7, but for the inverse 7-day annual minimum flows. Here, the results are more mixed, with the LP3 continuing to perform well, but the GEV and LN3 also performing well in many regions of the United States. In drier regions (e.g., Water Resources Regions 12, 13, and 15), which generally produce lower flows, the GEV appears to be as good as or perhaps better than the LP3 distribution. For larger values of skew, the GEV generally has a larger kurtosis than the other distribution; this thicker tailed distribution may better describe the inverse of low streamflows when smaller values are present in the record.

L-Moment Diagrams for Censored Flows

In low flow frequency analysis, the focus is generally on estimating a quantile in the lower tail of the distribution (unlike for flood frequency, where qauntiles are generally estimated in the upper tail). The larger observations, which are less important with these low flow quantiles, may impact the higher L-moments, the estimated parameters of the distribution, and thus the quantile estimates. Of interest is if one removes a percentage of the largest observations (i.e., censors the largest observations), whether the remaining observations will be more consistent with a particular probability distribution. This idea is analogous to the current approach to the removal of potentially influential low outliers in flood frequency analysis (Cohn et al. 2013). Hosking (1995) introduced two types of censoring for probability weighted moments: Type A and Type B. While Hosking (1995) only considered the case of censoring in the upper tail of the distribution, Zafirakou-Koulouris et al. (1998) extended the analysis to consider lower tail censoring. L-moment analysis for Type B censoring is performed when the censored observations are replaced by a nominal value, such as zero. Kroll and Vogel (2002) examined shifts in probability distributions for Type B censoring when some observations of the annual minimum series were recorded as zero. Type A censoring is equivalent to taking the L-moments of the uncensored observations. Here, Type A censoring is explored by censoring portions of the upper tail of the observed low streamflow series, calculating the L-moment ratios of the remaining observations, and comparing the observed censored L-moment ratios to the relationships of Type A censoring to different probability distributions.

To perform this analysis, the low flow series with no zeros were utilized. At each site, a certain percentage (25%, 50%, and 75%) of the largest observations were censored (i.e., removed) and L-moment ratios were calculated using the remaining observations. To develop relationships between τ_3 and τ_4 for each probability distribution with Type A censoring, a simulation experiment was performed. First, 100,000 random variables were generated for the respective distribution for a range of different distributional parameters. The 100,000 variables were then sorted and the largest 25%, 50%, or 75% of the values were censored (i.e., removed); τ_3 and τ_4 were then calculated for the remaining data, which represent the lower tail of the distribution.

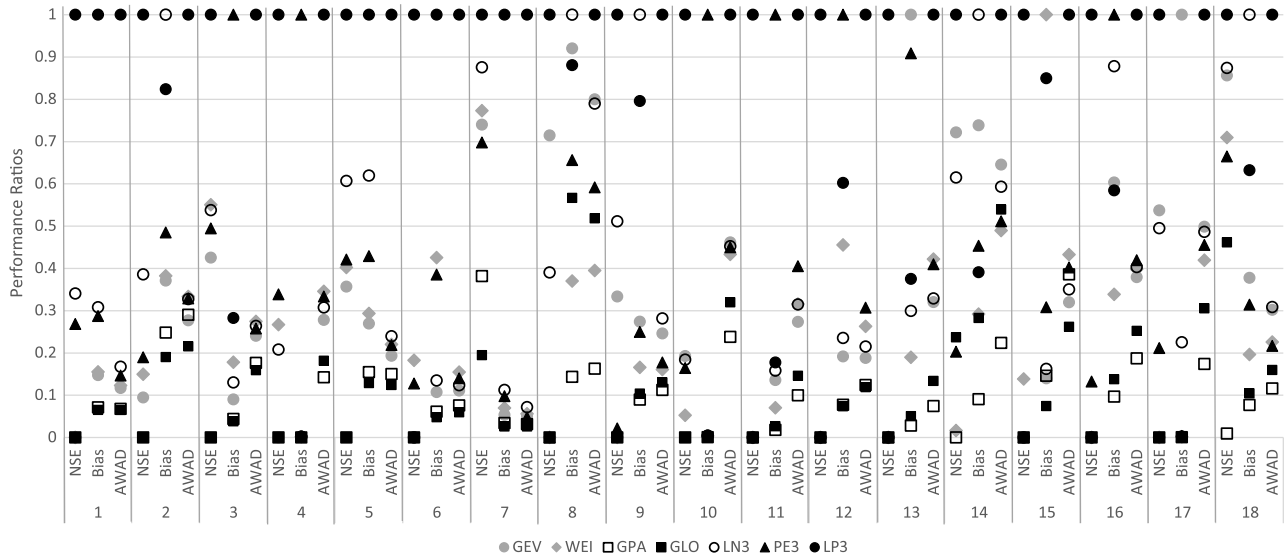

Fig. 7. Distributional performance ratios for low streamflow series in each Water Resource Region 1–18 with no zero flows for the 1-day, 3-day, 7-day, 30-day, Q90, Q95, and Q99 annual minimum series.

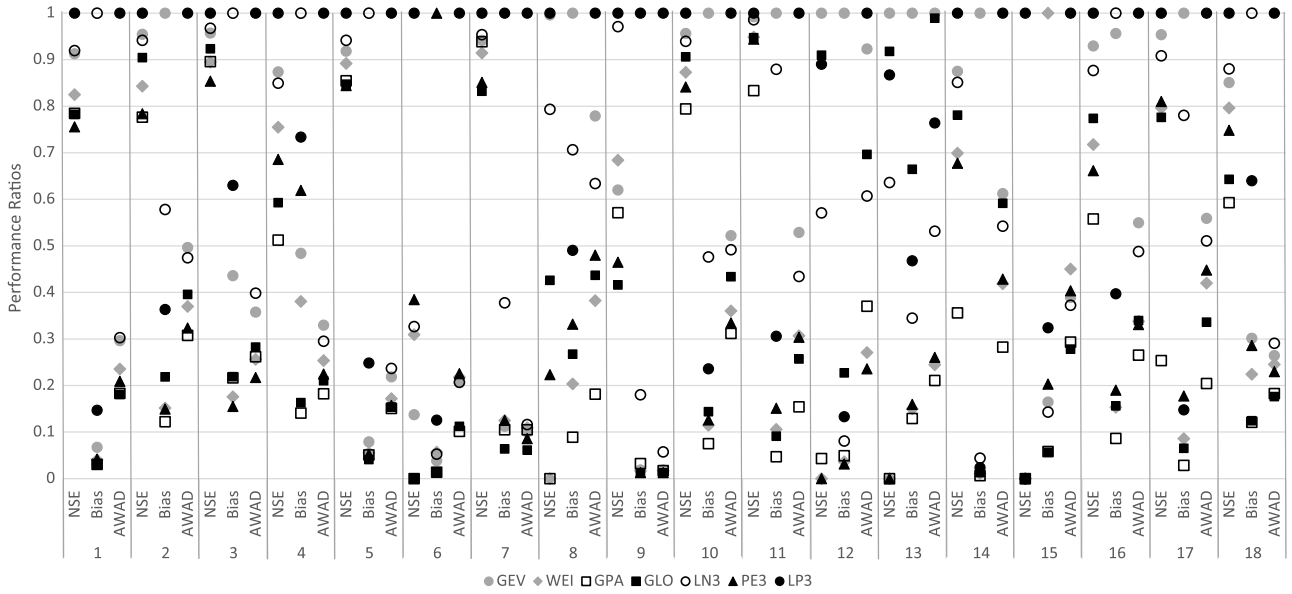

Fig. 8. Distributional performance ratios for low streamflow series in each Water Resource Region 1–18 with inverse of no zero flows for the 1-day, 3-day, 7-day, 30-day, Q90, Q95, and Q99 annual minimum series.

For each distribution and each censoring level, an ordinary least squares regression model of the form

$$\tau_4 = \sum_{k=0}^{8} A_k \tau_3^k \beta_0 \tag{7}$$

was then fit to the censored τ_3 and τ_4 values to develop an approximation of the theoretical τ_3:τ_4 relationship for each distribution at the upper tail censoring of 25%, 50%, and 75%. A similar method was employed by Hosking and Wallis (1997) and Zafirakou-Koulouris et al. (1998) to approximate L-moment ratio relationships for different uncensored distributions. The model was fit for a range of τ_3 from the minimum observed value across all sites to 0.9 based on maximizing the adjusted coefficient of determination. This was done for all distributions previously examined in this experiment except for LP3, which has an unusual uncensored τ_3:τ_4 relationship (an area as opposed to a line) that complicates the development of a censored approximation.

Fig. 9 contains a plot of τ_4 versus τ_3 of the untransformed 7-day annual minimums at sites with no zero flows for 25% censoring. This plot contained points for the observed τ_3 and τ_4 for sites with no zero 7-day annual minimums with Type A censoring as well as the approximation to the theoretical relationship for each distribution. Wang (1990) noted that the censored τ_3:τ_4 relationship for GEV distribution becomes shallower compared to the uncensored distribution and this was also observed for all of the distributions in the present study. As the censoring level increases, for positively skewed distributions, the τ_3 values decrease and the τ_4 value increases. This is because as the upper tail of these distributions is removed, the skew is reduced and the thickness of the tails increases. As censoring increased, the theoretical relationship between τ_3 and τ_4 becomes more similar for all distributions except the GPA. An interesting component of Fig. 9 is that most sites appear to cluster around a value of τ_3 equal to 0 (the average τ_3 and τ_4 across all sites is −0.010 and 0.063, respectively). Similar experiments were performed with censoring of the lower tail of the inverse flows (not shown here). In general, censoring of the upper tail of the distribution, or the lower tail of the distribution of the inverse flows, did not improve the fit of probability distributions to low streamflow series.

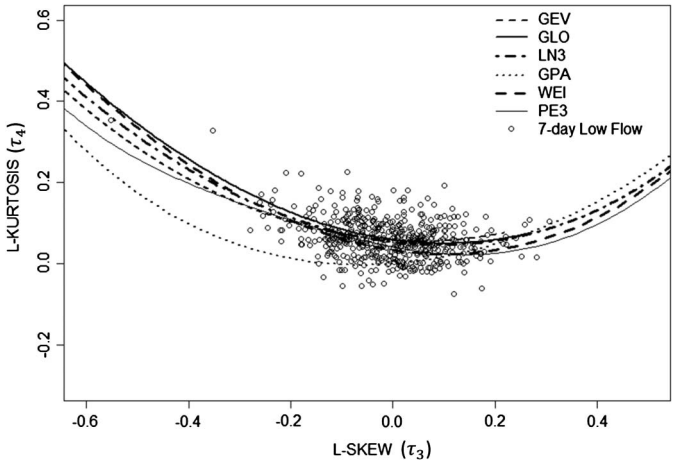

Fig. 9. τ_3 versus τ_4 with 25% censoring of the upper tail for 7-day annual minimum flows at HCDN-2009 sites with no zeros.

Closer Look at the LP3, GEV, and LN3 Distributions

From the analysis of L-moment diagrams for the untransformed and inverse low flow series at sites with no zero annual minimums, the most plausible 3-parameter distributions to describe low streamflow series in the US appear to be the LP3, GEV, LN3, and PE3 distributions. Here, a closer examination is provided of three of these distributions: LP3, GEV, and LN3. If a series is generated by the LP3 distribution, then the logarithm of that series should follow a PE3 distribution. Fig. 10(a) contains a plot of τ_4 versus τ_3 for the logarithm of the 7-day annual minimum series at the 495 sites with no zero 7-day annual minimums. The τ_3:τ_4 relationship for the PE3 distribution is also plotted in this figure. While the PE3 distribution line generally intersects the middle of the data points, there does not seem to be overwhelming evidence that the log of the series follows a PE3 distribution and thus, the untransformed series follows a LP3 distribution. In fact, the data seems to be centered on a τ_3 of 0 (and a τ_4 of 0.12), which is consistent with a 2-parameter

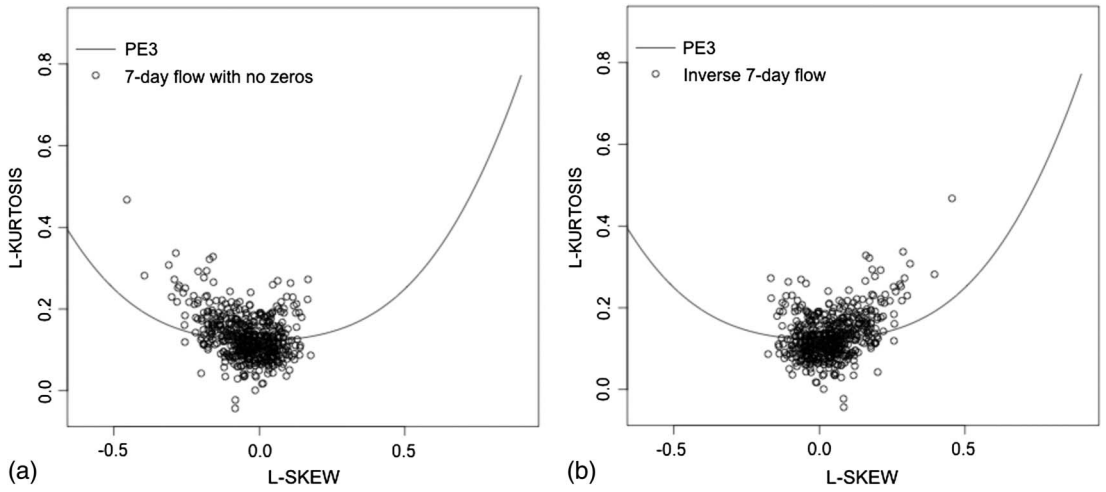

Fig. 10. τ_3 versus τ_4 for the logarithm of (a) 7-day annual minimum flows; and (b) the inverse of 7-day annual minimum flows at HCDN-2009 sites with no zeros.

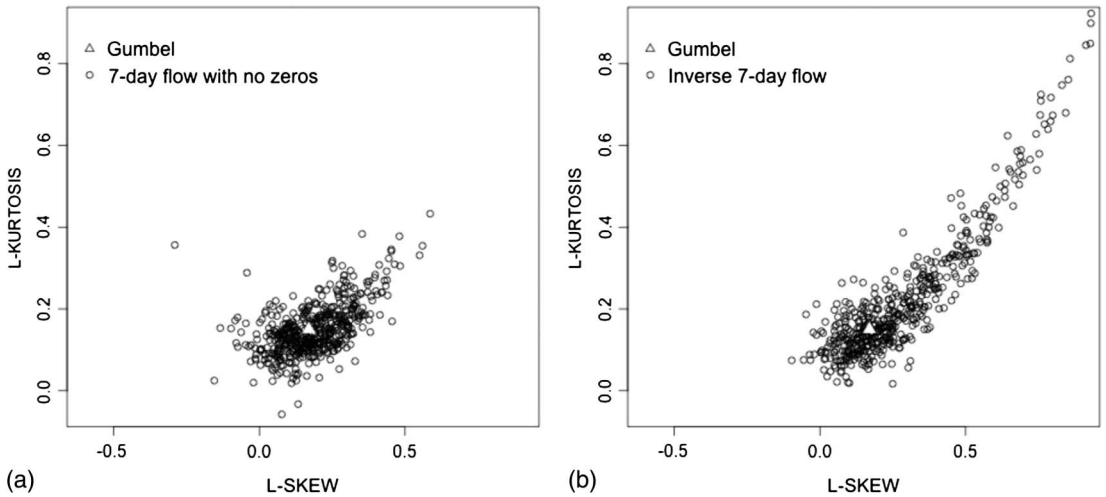

Fig. 11. τ_3 versus τ_4 for the logarithm of (a) 7-day annual minimum flows; and (b) the inverse of 7-day annual minimum flows after the lower bound of the Type II GEV distribution has been subtracted (or the data is subtracted from the upper bound of a Type III GEV distribution) at HCDN-2009 sites with no zeros.

lognormal distribution. A similar inverse pattern can be seen in Fig. 10(b) for the log of the inverse flows, which is just the mirror image of Fig. 10(a) since the $\log(1/x) = -\log(x)$.

If a series is generated by a GEV distribution, then if one subtracts the lower bound of a Type II GEV distribution from the data, or subtracts the data from the upper bound of a Type III GEV distribution, and takes the logarithm, the resulting data set follows a Gumbel distribution (Johnson and Kotz 1995). A Type II or Type III GEV distribution is distinguished by the sign of the shape parameter κ ($\kappa < 0$ for Type II and $\kappa > 0$ for Type III). Fig. 11(a) contains a plot of τ_4 versus τ_3 for the logarithm of the 7-day annual minimum series after this transformation for the 495 sites with no zero 7-day annual minimums. The parameters of the GEV distribution were estimated using the method of L-moments (Hosking and Wallis 1997). The τ_3:τ_4 relationship for the Gumbel distribution, which is a point on this plot, is also plotted on this figure. All of the L-moment ratios in Fig. 11(a) appear to cluster around the theoretical value for a Gumbel distribution so that it is entirely possible that the untransformed data arise from a GEV distribution. The lower bound of the GEV distribution is a function of κ, the shape parameter. The GEV distribution is very sensitive to κ and generally, a regional κ is recommended (Chowdhury et al. 1991). Since here the region is the conterminous US, an at-site κ is employed, which introduces more uncertainty into this analysis and may be why there is more variability in the L-moment ratios in Fig. 11(a) than is to be expected. Fig. 11(b) is the same as Fig. 11(a), but for the inverse of the 7-day annual minimums; for the inverse flows, even larger at-site L-moment ratios are observed. The conclusion derived from Fig. 11(b) is that it is unlikely that the inverse flows arise from a GEV distribution.

If a series is generated by a LN3 distribution, and the lower bound of the LN3 distribution is subtracted from the series, then the logarithm of the resulting data set should follow a normal distribution. Fig. 12(a) contains τ_4 versus τ_3 for the logarithm of the 7-day annual minimum series after the lower bound of the LN3 distribution has been subtracted at the 495 sites with no zero 7-day annual minimums. For consistency, the lower bound of the LN3 distribution was estimated using the method of L-moments

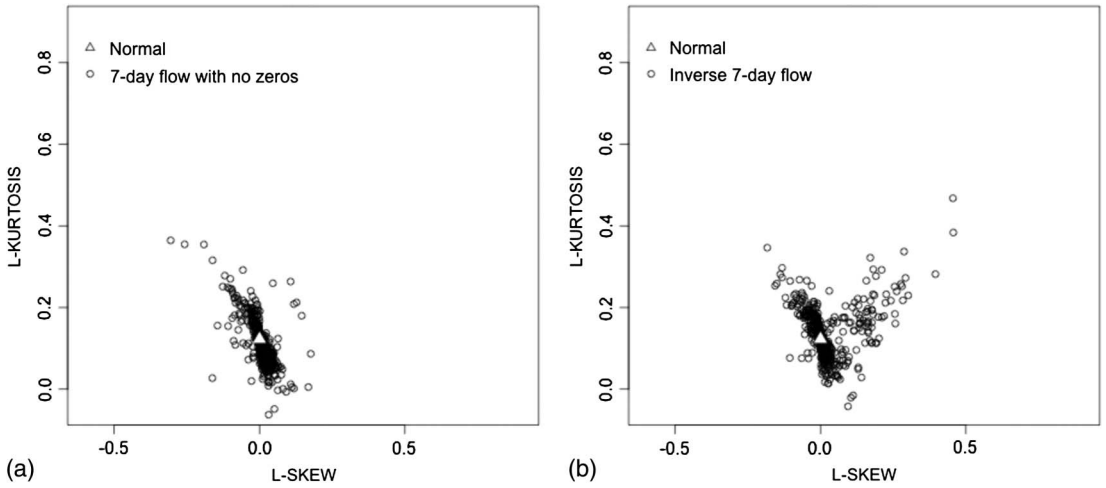

Fig. 12. τ_3 versus τ_4 for the logarithm of (a) 7-day annual minimum flows; and (b) the inverse of 7-day annual minimum flows after the lower bound of the LN3 distribution has been subtracted at HCDN-2009 sites with no zeros.

(Hosking and Wallis 1997). The τ_3:τ_4 relationship for the normal distribution, which is a point on this plot, is also plotted on the figure. The normal distribution point on Fig. 12(a) falls within the cluster of data points and the data points appear to be more tightly clustered around this point than was observed for the LP3 or GEV distributions in Figs. 8 and 9. Fig. 12(b) contains the same plot, but for the inverse of the 7-day annual minimum flows. The patterns of the L-moment ratios in Fig. 12 do not take on the type of elliptical shapes expected if the untransformed observations arose from an LN3 distribution, which may be due to the variability introduced by having to estimate the lower bound of the distribution.

Conclusion

In this study, L-moment diagrams of L-kurtosis (τ_4) versus L-skew (τ_3) were constructed for seven low streamflow series commonly employed in the practice of low flow frequency analyses: the 1-day, 3-day, 7-day, and 30-day annual minimum flows, and annual flow duration curve quantiles with exceedance probabilities of 90%, 95%, and 99%. For each of these series, L-moment ratios were estimated at 704 unregulated HCDN-2009 gaging stations located in the contiguous US with record lengths ranging from 28 to 117 years. L-moment diagrams were used to assess the goodness of fit of seven 3-parameter probability distributions: GEV, GLO, GPA, LN3, LP3, PE3, and WEI. The visual assessment of L-moment diagrams was combined with the calculation of goodness of fit statistics based on the relationship between the values of τ_4 according to the observations and values of τ_4 derived from the fitted distributions. The three goodness of fit statistics were the record-length weighted NSE, bias, and average weighted absolute distance (AWAD).

Studies have shown that sites with and without annual minimums of zero lead to differences in probabilistic behavior. Sites with more zeros produce higher L-skew values. For this study, a distinction was made between sites that recorded annual minimum flows as zeros and those that did not. To assess the goodness of fit of different probability distributions, both the original untransformed low flow series and the inverse of the low flow series for sites without zeros were analyzed. The sites without zeros were also censored by removing the largest 25%, 50%, and 75% of the data, and the L-moment ratios for this censored data were compared to the L-moment ratios for censored probability distributions.

The results indicated that the LP3 distribution was plausible for all the low flow series, regardless of whether the series had zeros, no zeros, or the inverse was analyzed. Since the τ_3:τ_4 relationship for the LP3 is an area and not a curve as it is for the other distributions considered, the LP3 had an inherently unfair advantage over the other distributions. Yet, the fact that the LP3 occupies a region rather than a curve in the L-moment diagram is because it is a more flexible distribution than nearly all other 3-parameter distributions. For low flow series with no zeros, the LN3 and PE3 are also plausible distributions, and for low flow series with zeros, the WEI and PE3 appear to be plausible. For the inverse of nonzero flows, the results favored the LN3 and GEV in addition to the LP3. In general, an inverse transformation of the flows produces L-moment diagrams with a larger range of L-skew and L-kurtosis than the untransformed flows, and the distributions fit similarly to both the inverse and untransformed flows. Fitting a probability distribution to the inverse of the low flows removes the possibility of estimating negative low flow quantiles, which can be a problem in practice when fitting real-space distributions. Censoring of the upper tail of the distribution generally made it harder to assess the goodness of fit.

Based on the results, the following conclusions can be drawn:

1. The LP3 generally performed best for all series (with zeros, no zeros, and the inverse low flow series), though the LN3 and PE3 are plausible distributions for sites with no zero flows.
2. The inverse of nonzero low flow series produces L-moment ratio diagrams in which the LP3, GEV, and LN3 distributions appear most plausible. Further investigation of fitting probability distributions to the inverse of low flow series may be warranted, especially when applying real-space probability distributions that may generate negative quantile estimates.
3. Given that the GEV distribution is often considered the distribution of choice for all extreme value applications due to its foundation in the theory of extremes, it is of considerable interest that this distribution is one of the recommended distributions for fitting the series of nonzero low flow series. Future research should perform comparative assessment of the sampling properties of estimated quantiles derived from fitting a GEV distribution to the inverse of the low flow series in contrast with fitting, for example, an LP3, LN3, or PE3 distribution to the untransformed series.

Acknowledgments

The authors are grateful to the State University of New York College of Environmental Science and Forestry (SUNY-ESF), the International Institute of Education (IIE), the US Department of State's Bureau of Educational and Cultural Affairs (ECA), and the United States Educational Foundation in Pakistan for funding provided through the Fulbright Scholarship Program that supported this research.

References

AMS (American Meteorological Society). 1997. "Meteorological drought-policy statement." *Bull. Am. Meteorol. Soc.* 78 (5): 847–852. https://doi.org/10.1175/1520-0477-78.5.847.

Armentroutand, G. W., and J. F. Wilson. 1987. *Assessment of low flows in streams in northeastern Wyoming*. USGS Water-Resources Investigations Rep. No. 85-4246. Washington, DC: USGS.

Atkins, J. B., and J. L. Pearman. 1995. *Low-flow and flow-duration characteristics of Alabama streams*. USGS Water-Resources Investigations Rep. No. 93-4186. Washington, DC: USGS.

Barnes, C. R. 1986. *Method for estimating low-flow statistics for ungaged streams in the lower Hudson River Basin*. USGS Water-Resources Investigations Rep. No. 85-4070. Washington, DC: USGS.

Blum, A. G., S. A. Archfield, and R. M. Vogel. 2017. "On the probability distribution of daily streamflow in the United States." *Hydrol. Earth Syst. Sci.* 21 (6): 3093–3103. https://doi.org/10.5194/hess-21-3093-2017.

Caruso, B. S. 2000. "Evaluation of low-flow frequency analysis methods." *J. Hydrol. (NZ)* 39 (1): 19–47.

Chen, Y. D., G. Huang, Q. Shao, and C. Y. Xu. 2010. "Regional analysis of low flow using L-moments for Dongjiang basin, South China." *Hydrol. Sci. J.* 51 (6): 1051–1064. https://doi.org/10.1623/hysj.51.6.1051.

Chowdhury, J., J. R. Stedinger, and L. H. Lu. 1991. "Goodness-of-fit tests for regional generalized extreme value flood distributions." *Water Resour. Res.* 27 (7): 1765–1776. https://doi.org/10.1029/91WR00077.

Cohn, T. A., J. F. England, C. E. Berenbrock, R. R. Mason, J. F. Stedinger, and J. R. Lamontagne. 2013. "A generalized Grubbs-Beck test statistic for detecting multiple potentially influential low outliers in flood series." *Water Resour. Res.* 49: 5047–5058. https://doi.org/10.1002/wrcr.20392.

Dodangeh, E., M. T. Sattari, and N. Seçkin. 2011. "Regional frequency analysis of minimum flow by L-moments method." *Tarim Bilimleri Dergisi* 17 (1): 43–58.

Dodangeh, E., S. Soltani, A. Sarhadi, and J. T. Shiau. 2013. "Application of L-moments and Bayesian inference for low-flow regionalization in Sefidroud basin, Iran." *Hydrol. Processes* 28 (4): 1663–1676. https://doi.org/10.1002/hyp.9711.

England, J. F., T. A. Cohn, B. A. Faber, J. R. Stedinger, W. O. Thomas, A. G. Veilleux, J. E. Kiang, and R. R. Mason. 2018. *Guidelines for determining flood flow frequency—Bulletin 17C (ver. 1.1, May 2019): USGS techniques and methods*. Washington, DC: USGS. https://doi.org/10.3133/tm4B5.

Falcone, J. A. 2011. "GAGES-II, geospatial attributes of gages for evaluating streamflow." Accessed January 15, 2018. http://water.usgs.gov/GIS/metadata/usgswrd/XML/gagesII_Sept2011.xml.

FAO (Food and Agricultural Organization). 2017. *The future of food and agriculture: Trends and challenges*. Rome: FAO.

Farmer, W. H., T. M. Over, and R. M. Vogel. 2015. "Multiple regression and inverse moments improve the characterization of the spatial scaling behavior of daily streamflows in the Southeast United States." *Water Resour. Res.* 51 (3): 1775–1796. https://doi.org/10.1002/2014WR015924.

Filliben, J. J. 1975. "The probability plot correlation coefficient test for normality." *Technometrics* 17 (1): 111–117. https://doi.org/10.1080/00401706.1975.10489279.

Gao, S., P. Liu, Z. Pan, B. Ming, S. Guo, and L. Xiong. 2017. "Derivation of low flow frequency distributions under human activities and its implications." *J. Hydrol.* 549 (Jun): 294–300. https://doi.org/10.1016/j.jhydrol.2017.03.071.

Goda, Y., M. Kudaka, and H. Kawai. 2011. "Incorporation of Weibull distribution in L-moments method for regional frequency analysis of peaks-over-threshold wave heights." *Coastal Eng. Proc.* 1 (32): 1–11.

Griffis, V. W., and J. R. Stedinger. 2007. "Log-Pearson type 3 distribution and its application in flood frequency analysis. I: Distribution characteristics." *J. Hydrol. Eng.* 12 (5): 482–491. https://doi.org/10.1061/(ASCE)1084-0699(2007)12:5(482).

Guttman, N. B., J. R. M. Hosking, and J. R. Wallis. 1993. "Regional precipitation quantile values for the continental United States computed from L-moments." *J. Clim.* 6 (12): 2326–2340. https://doi.org/10.1175/1520-0442(1993)006<2326:RPQVFT>2.0.CO;2.

Hosking, J. R. M. 1995. "The use of l-moments in the analysis of censored data." In *Recent advances in life-testing and reliability*, 545–564. Boca Raton, FL: CRC Press.

Hosking, J. R. M. 2017. "Package 'lmom' (version 2.6)." Accessed September 15, 2017. https://cran.r-project.org/web/packages/lmom/lmom.pdf.

Hosking, J. R. M., and J. R. Wallis. 1993. "Some statistics useful in regional frequency analysis." *Water Resour. Res.* 29 (2): 271–281. https://doi.org/10.1029/92WR01980.

Hosking, J. R. M., and J. R. Wallis. 1997. *Regional frequency analysis: An approach based on L-moments*. Cambridge, UK: Cambridge University Press.

Howitt, R., D. MacEwan, J. Medellin-Azuara, J. Lund, and D. Sumner. 2015. *Economic analysis of the 2015 drought for California Agriculture*, 16. Davis, CA: Center for Watershed Sciences, Univ. of California–Davis.

Hughes, G. H. 1981. "*Low-flow frequency data for selected stream gaging stations in Florida*." USGS Open-File Rep. No. 81-69. Washington, DC: US Dept. of the Interior, USGS.

Hussain, Z. 2011. "Application of the regional flood frequency analysis to the upper and lower basins of the Indus River, Pakistan." *Water Resour. Manage.* 25 (11): 2797–2822. https://doi.org/10.1007/s11269-011-9839-5.

Hussain, Z. 2017. "Estimation of flood quantiles at gauged and ungauged sites of the four major rivers of Punjab, Pakistan." *Nat. Hazard.* 86 (1): 107–123. https://doi.org/10.1007/s11069-016-2676-3.

Johnson, N. L., and S. Kotz. 1995. "Extreme value distributions." In *Continuous university distributions*, 1–112. Hoboken, NJ: Wiley.

Keshtkar, A. R. 2015. "Low flow frequency analysis by L-moments method. Case study: Iranian central plateau river basin." *Desert* 20 (2): 167–175.

Kim, D. Y., S. H. Lee, Y. J. Hong, E. J. Lee, and S. J. Im. 2010. "The determination of probability distributions of annual, seasonal, and monthly precipitation in Korea." *Korean J. Agric. For. Meteorol.* 12 (2): 83–94. https://doi.org/10.5532/KJAFM.2010.12.2.083.

Kroll, C. N., and R. M. Vogel. 2002. "Probability distribution of low streamflow series in the United States." *J. Hydrol. Eng.* 7 (2): 137–146. https://doi.org/10.1061/(ASCE)1084-0699(2002)7:2(137).

Lin, H. F. 2012. *USGS hydro-climatic data network 2009 (HCDN-2009)*. USGS Fact Sheet 2012-3047. Washington, DC: USGS.

Modarres, R. 2008. "Regional frequency distribution type of low flow in north of Iran by L-moments." *Water Resour. Manage.* 22 (7): 823–841. https://doi.org/10.1007/s11269-007-9194-8.

NOAA-NCEI (National Oceanic and Atmospheric Administration-National Centers for Environmental Information). 2018. "U.S. billion-dollar weather and climate disasters." Accessed June 2, 2018. https://www.ncdc.noaa.gov/billions.

Pearson, C. P. 1991. "New Zealand regional flood frequency analysis using L-moments." *N. Z. Hydrol. Soc.* 30 (2): 53–64.

Pearson, C. P. 1995. "Regional frequency analysis of low flows in New Zealand Rivers." *J. Hydrol. (NZ)* 33 (2): 94–122.

Peng, S., C. Xi, Q. Si-min, Z. Zhi-cai, and M. Jian-liang. 2010. "Regional frequency analysis of low flow based on L moments: Case study in Karst Area, Southwest China." *J. Hydrol. Eng.* 15 (5): 370–377. https://doi.org/10.1061/(ASCE)HE.1943-5584.0000206.

Riggs, H. C. 1980. "Characteristics of low flows." *J. Hydraul. Div.* 106 (5): 717–731.

Rossman, L. A. 1990. "Design stream flows based on harmonic means." *J. Hydrol. Eng.* 7 (116): 946–950. https://doi.org/10.1061/(ASCE)0733-9429(1990)116:7(946).

Sankarasubramanian, A., and K. Srinivasan. 1999. "Investigation and comparison of sampling properties of L-moments and conventional moments." *J. Hydrol.* 218 (1): 13–34. https://doi.org/10.1016/S0022-1694(99)00018-9.

Smakhtin, V. U. 2001. "Low flow hydrology: A review." *J. Hydrol.* 240 (3): 147–186. https://doi.org/10.1016/S0022-1694(00)00340-1.

Stedinger, J. R., R. M. Vogel, and E. Foufoula-Georgiou. 1993. "Frequency analysis of extreme events." In *Handbook of hydrology*. New York: McGraw-Hill.

Tasker, G. D. 1989. "Regionalization of low flow characteristics using logistic and GLS regression." In *New directions for surface water modeling*, 181. London: IAHS Publication.

VanLoon, A. F. 2015. "Hydrological drought explained." *Wiley Interdiscip. Rev.: Water* 2 (4): 359–392. https://doi.org/10.1002/wat2.1085.

Vogel, R. M., and N. M. Fennessey. 1993. "*L* moment diagrams should replace product moment diagrams." *Water Resour. Res.* 29 (6): 1745–1752. https://doi.org/10.1029/93WR00341.

Vogel, R. M., and C. N. Kroll. 1989. "Low flow frequency analysis using probability-plot correlation coefficients." *J. Water Resour. Plann. Manage.* 115 (3): 338–357. https://doi.org/10.1061/(ASCE)0733-9496(1989)115:3(338).

Vogel, R. M., and I. Wilson. 1996. "Probability distribution of annual maximum, mean, and minimum streamflows in the United States." *J. Hydrol. Eng.* 1 (2): 69–76. https://doi.org/10.1061/(ASCE)1084-0699(1996)1:2(69).

Wang, Q. 1990. "Estimation of the GEV distribution from censored samples by method of partial probability weighted moments." *J. Hydrol.* 120 (1–4): 103–114. https://doi.org/10.1016/0022-1694(90)90144-M.

Wang, W., X. G. Wang, and X. Zhou. 2011. "Impacts of Californian dams on flow regime and maximum/minimum flow probability distribution." *Hydrol. Res.* 42 (4): 275–289. https://doi.org/10.2166/nh.2011.137.

Yue, S., and C. Y. Wang. 2004. "Possible regional probability distribution type of Canadian annual streamflow by L-moments." *Water Resour. Manage.* 18 (5): 425–438. https://doi.org/10.1023/B:WARM.0000049145.37577.87.

Zafirakou-Koulouris, A., R. M. Vogel, S. M. Craig, and J. Habermeier. 1998. "L-moment diagrams for censored observations." *Water Resour. Res.* 34 (5): 1241–1249. https://doi.org/10.1029/97WR03712.

Zalants, M. G. 1992. *Low-flow frequency and flow duration of selected South Carolina streams through 1987*. USGS Water-Resources Investigations Rep. No. 91-4170. Washington, DC: USGS.

Zou, L., J. Xia, and D. She. 2018. "Analysis of impacts of climate change and human activities on hydrological drought: A case study in the Wei River Basin, China." *Water Resour. Manage.* 32 (4): 1421–1438. https://doi.org/10.1007/s11269-017-1877-1.